

Effect of Natural Organic Matter on the Fate of Cadmium During Microbial Ferrihydrite Reduction

Zhe Zhou,* E. Marie Muehe, Elizabeth J. Tomaszewski, Juan Lezama-Pacheco, Andreas Kappler, and James M. Byrne



Cite This: *Environ. Sci. Technol.* 2020, 54, 9445–9453



Read Online

ACCESS |



Metrics & More

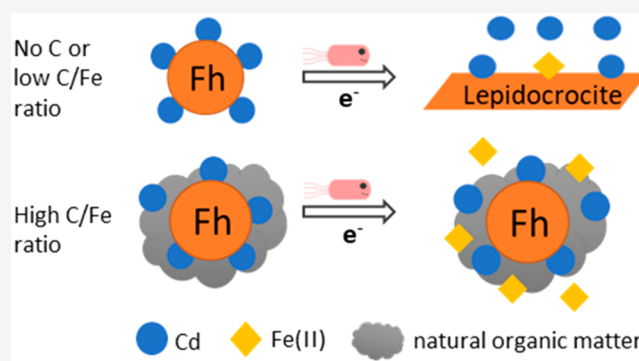


Article Recommendations



Supporting Information

ABSTRACT: Natural organic matter (NOM) is known to affect the microbial reduction and transformation of ferrihydrite, but its implication toward cadmium (Cd) associated with ferrihydrite is not well-known. Here, we investigated how Cd is redistributed when ferrihydrite undergoes microbial reduction in the presence of NOM. Incubation with *Geobacter sulfurreducens* showed that both the rate and the extent of reduction of Cd-loaded ferrihydrite were enhanced by increasing concentrations of NOM (i.e., C/Fe ratio). Without NOM, only 3–4% of Fe(III) was reduced, but around 61% of preadsorbed Cd was released into solution due to ferrihydrite transformation to lepidocrocite. At high C/Fe ratio (1.6), more than 35% of Fe(III) was reduced, as NOM can facilitate bioreduction by working as an electron shuttle and decreased aggregate size, but only a negligible amount of Cd was released into solution, thus decreasing Cd toxicity and prolonging microbial Fe(III) reduction. No ferrihydrite transformation was observed at high C/Fe ratios using Mössbauer spectroscopy and X-ray diffraction, and X-ray absorption spectroscopy indicated the proportion of Cd-OM bond increased after microbial reduction. This study shows that the presence of NOM leads to less mobilization of Cd under reducing condition possibly by inhibiting ferrihydrite transformation and recapturing Cd through Cd-OM bond.



INTRODUCTION

Ferrihydrite, a short-range ordered Fe(III) oxyhydroxide, is widely distributed in soils and sediments.^{1,2} Its association with cadmium (Cd), one of the major contaminants in agricultural soils, has been shown to decrease the mobility and bioavailability of Cd.^{3–5} However, ferrihydrite is not stable under reducing conditions where it can undergo reductive transformation,^{6,7} raising the question about how stable Cd is when associated with ferrihydrite.

Ferrihydrite can be reduced to Fe(II) via abiotic or microbial processes in anoxic environments.^{8–10} The formed Fe(II) either remains in solution as aqueous Fe²⁺, precipitates as secondary Fe(II) minerals,^{11,12} or reacts with remaining ferrihydrite and transforms it into secondary Fe minerals.^{6,13} With the reductive dissolution of Fe(III), Cd associated with ferrihydrite can be first released into solution due to the loss of adsorption sites.¹⁴ But with continuous Fe(II) production by microbial reduction and suitable geochemical conditions, the released Cd can be reimmobilized through the precipitation of Fe(II) or Fe(II)/Fe(III) mixed minerals,^{15,16} or readsorbed by secondary Fe minerals.^{17,18} In the natural environment, it is difficult to predict the fate of Cd during microbial ferrihydrite reduction as other natural components, such as NOM,¹⁹ may also associate with ferrihydrite and change its behavior.

NOM, associated with ferrihydrite through adsorption or coprecipitation, is known to affect ferrihydrite microbial reduction and its transformation pathways depending on the C/Fe ratios.^{20–22} From the perspective of microbial reduction, NOM resulted in slower ferrihydrite reduction rate at low C/Fe ratios compared to pure ferrihydrite, while enhanced the extent of reduction at higher C/Fe ratios.^{11,20} It has been shown that NOM can impact microbial ferrihydrite reduction by (1) complexation of Fe(II) and Fe(III), thus changing the redox potential and the solubility of surface Fe(III),^{23,24} (2) altering ferrihydrite particle aggregation depending on NOM concentrations thereby changing ferrihydrite accessibility for Fe(III)-reducing bacteria,²⁵ and (3) working as an electron shuttle between cells and Fe(III) minerals.^{26,27} Furthermore, NOM at high C/Fe ratios was suggested to constrain ferrihydrite crystal growth through Ostwald ripening or oriented aggregation, resulting in a lack of ferrihydrite

Received: May 12, 2020

Revised: June 15, 2020

Accepted: July 7, 2020

Published: July 7, 2020



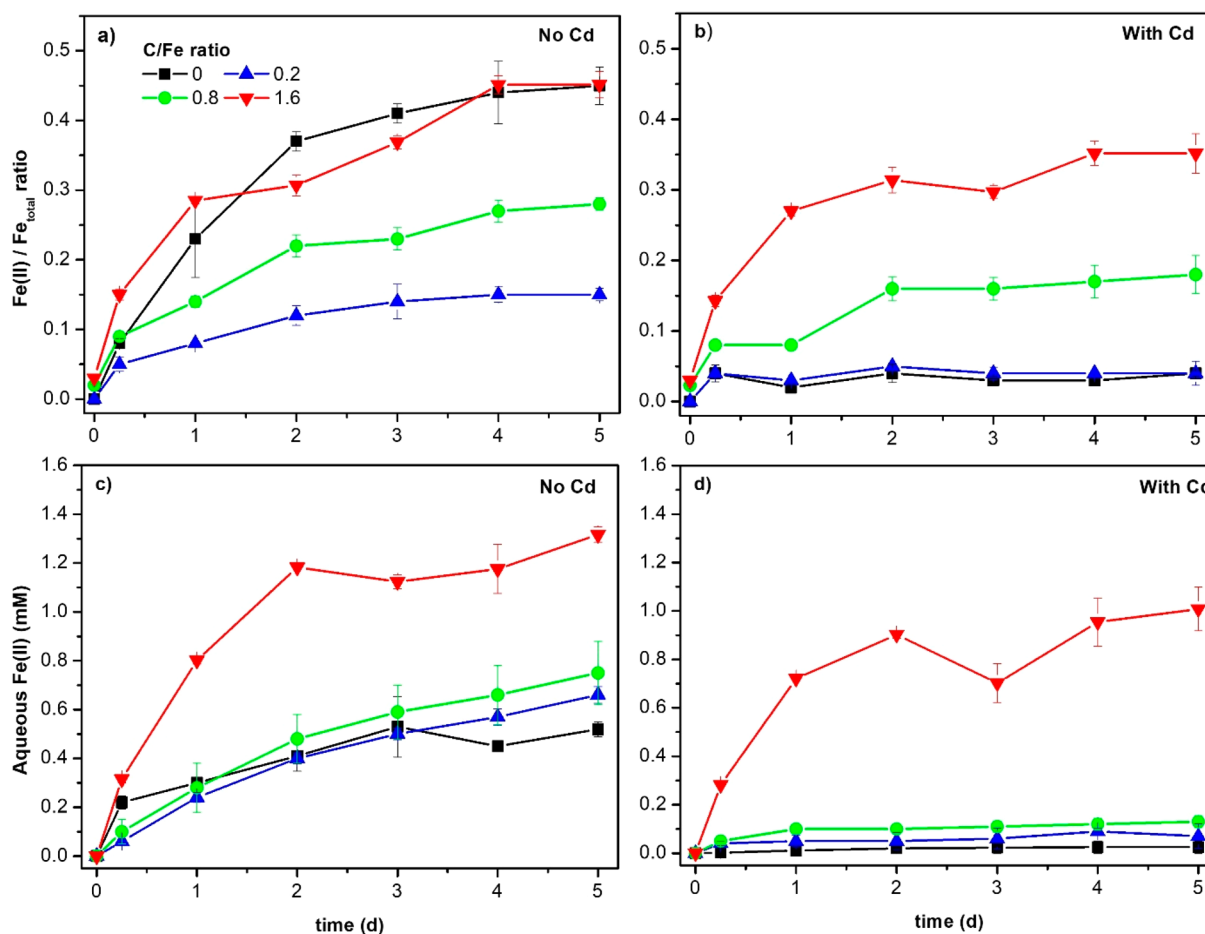


Figure 1. Ratio of Fe(II)/total Fe (a, b) and aqueous Fe²⁺ concentration (c, d) during microbial reduction (*G. sulfurreducens*) of ferrihydrite and Cd-loaded ferrihydrite in the presence of SRNOM at different C/Fe ratios. Data represent the mean and standard deviation measured in triplicate bottles.

transformation.^{28,29} In general, NOM can facilitate microbial ferrihydrite reduction at high C/Fe ratios but inhibit ferrihydrite transformation, raising a question about its implication for associated Cd. To date, however, little is known about the effect of NOM on the fate of Cd during microbial Cd-loaded ferrihydrite reduction.

The main objective of this study therefore was to get a better understanding of the stability of Cd during microbial reduction of ferrihydrite under complex environmentally relevant conditions. Specifically, we investigated the role of NOM in this process and incubated ferrihydrite with adsorbed Cd and different amounts of NOM using Fe(III)-reducing bacteria *Geobacter sulfurreducens* (*G. sulfurreducens*). Fe(III) reduction, Fe mineralogy change, and Cd stability during microbial reduction were monitored through multiple characterization methods including scanning electron microscopy (SEM), X-ray diffraction (XRD), and Mössbauer and synchrotron-based X-ray absorption spectroscopy (Cd K-edge).

MATERIALS AND METHODS

Starting Material Preparation. Ferrihydrite was synthesized by neutralizing 0.1 M Fe(NO₃)₃ solution with 1 M KOH as described by Schwertmann and Cornell.³⁰ The precipitated ferrihydrite was centrifuged and washed 3 times with deionized water, and then resuspended by shaking and ultrasonic application. The ferrihydrite stock suspension was stored anoxically at 4 °C and used within 1 month. Suwannee River

natural organic matter (SRNOM), and Pahokee Peat humic acid (PPHA) were purchased from the International Humic Substance Society (IHSS) and dissolved in DI water at pH 9.0 (adjusted with 1 M NaOH) to make concentrated stock solutions. The carbon concentration in the stock solution was measured with a TOC analyzer (highTOC II, elemental, Germany).

G. sulfurreducens was obtained from the laboratory stock and precultured in anoxic bicarbonate-buffered (30 mM, pH 7.0) medium containing nutrients and vitamins as previously described.³¹ Fresh medium was inoculated with 10% v/v from the preculture, cells were grown to the early stationary phase (after 2-day growth) and then harvested by centrifugation at 5000 rpm (20 min, 10 °C), and washed twice using 10 mM PIPES buffer to remove phosphate and carbonate in the precultural medium. The cell density (cells mL⁻¹) in the stock was measured with an Attune NxT flow cytometry (Thermo Fisher Scientific), and the cells were used within 2 h.

Experimental Setup and Sampling. Experiments were set up in triplicates and conducted under sterile and anoxic conditions. 11.2 mg/L (0.1 mM) Cd and 5 mM sodium acetate were added to 10 mM PIPES buffer (pH 7.0). Sodium acetate worked as an easily bioavailable C source (electron donor) that is preferred by *G. sulfurreducens*. No Cd precipitation would be formed under this condition based on the analysis of Visual-MINTEQ. Varying amounts of NOM stock solution were then added to obtain 0, 17, 70, and 140

mgC/L prior to the addition of ferrihydrite (7 mM Fe(III)). The C/Fe molar ratios of each setup were 0, 0.2, 0.8 and 1.6, respectively. Cd, NOM, and ferrihydrite were equilibrated on a shaking bed in the dark for 1 day before the addition of bacteria. Control groups without Cd and bacteria were also prepared.

Bacteria were added from the *G. sulfurreducens* stock to obtain about 8×10^7 cells/mL (8×10^{-5} g/mL, 6.8×10^{10} cells/g ferrihydrite) in each bottle which were then incubated in the dark at 25 °C over 5 days. The D/L stain was used for some setup and we found around 70% of cells still intact after 5 days incubation (data not shown). To measure the overall ratio of Fe(II)/total Fe at each sample time point, 100 μ L sample was taken and dissolved in 900 μ L 6 M HCl, and diluted with 500 μ L anoxic DI water to avoid O₂ oxidation of Fe(II) in concentrated acid.³² We centrifuged 900 μ L sample (8385g, 1 min), and extracted supernatant for aqueous Fe(II) and aqueous Cd concentration measurement. The centrifuged solid was resuspended in 900 μ L of 0.1 M sodium acetate (pH 4.0) and left for 30 min for a mild extraction of adsorbed Cd. All Cd samples were diluted with 2% HNO₃ (Trace metal grade). All Fe samples were preserved in the dark and measured immediately.

Sample Analysis. Fe(II) and total Fe in aqueous samples were quantified in triplicate using the ferrozine assay.³³ Aqueous and extracted Cd concentrations were measured using microwave plasma-atomic emission spectrometer (MP-AES, Agilent). UV-vis spectroscopy (Specord 50, Analytik Jena) was applied to track the change in aqueous NOM concentration.³⁴ SEM samples were prepared as described previously,³¹ and the micrographs were collected using a JEOL JSM-6500F field emission SEM. Incubated ferrihydrite with different amount of Cd and SRNOM were dried in an anoxic glovebox and characterized with a μ -XRD (Bruker D8, Germany) equipped with a Co-K α (1.7903 Å) X-ray tube. The measurement was conducted at 30 kV/30 mA from 5° to 70°. Mössbauer spectroscopy samples were prepared by collecting solid with 0.45 μ m paper filter and sealing it anoxically between two pieces of Kapton tape. Mössbauer spectra were obtained with a standard transmission setup (Wissel, Wissenschaftliche Elektronik GmbH) using a ⁵⁷Co/Rh source. Sample temperatures were varied between 77 K and 5 K, controlled with a closed-cycle cryostat (SHI-850-I, Janis Research Co). The spectra were calibrated with α -⁵⁷Fe⁰ at 295 K and fitted using the Voigt based fitting (VBF) routine in the Recoil software (University of Ottawa, Canada).³⁵ X-ray absorption spectroscopy (XAS) was conducted at beamline 11-2 at Stanford Synchrotron Radiation Lightsource (SSRL), detailed information can be found in the [Supporting Information \(SI\)](#).

RESULTS AND DISCUSSION

Microbial Fe(III) Reduction. We first investigated the effect of NOM on microbial ferrihydrite reduction in the absence of Cd. *G. sulfurreducens* (approximately 8×10^7 cells/mL, 6.8×10^{10} cells/g ferrihydrite) was added to ferrihydrite with different amounts of adsorbed SRNOM at pH 7.0. An increased percentage of Fe(II)/Fe_{total} was measured over time in all setups, but the rate and extent varied with different C/Fe ratios ([Figure 1a](#) and [Table S1](#)). In the first 6 h of incubation, the Fe(III) reduction rate of pure ferrihydrite (i.e., C/Fe ratio of 0) was 45.6 ± 2.6 μ mol/d, compared to 26.4 ± 5.3 μ mol/d at a C/Fe ratio of 0.2. Further increasing the C/Fe ratio to 1.6

increased the Fe(III) reduction rate to 74.4 ± 2.4 μ mol/d. This observation is consistent with published studies where NOM was found to impede Fe(III) reduction at low C/Fe ratios but improve Fe(III) reduction at high C/Fe ratios.^{9,25}

To investigate the effect of SRNOM on microbial reduction of Cd-loaded ferrihydrite, ferrihydrite with adsorbed Cd and various amounts of SRNOM were incubated with *G. sulfurreducens* under the same conditions as above. The pH changed slightly between different bottles in the range of 7.0–7.2 after microbial incubation. At a C/Fe ratio of 0, the presence of Cd greatly impeded microbial ferrihydrite reduction with only around 3–4% of Fe(III) reduced over 5 days incubation, and most of the reduction occurring in the first 6 h. Similar microbial Fe(III) reduction was observed at the C/Fe ratio of 0.2. The percentage of Fe(III) reduction over 5 days increased to $18 \pm 3\%$ at a C/Fe ratio of 0.8 and $35 \pm 3\%$ at a C/Fe ratio of 1.6. A faster average Fe(III) reduction rate was found at higher C/Fe ratios, especially in the first 6 h of incubation ([Table S1](#)). During the microbial reduction of Fe(III), there was no obvious SRNOM release measured by UV-vis spectra in all setups. The presence of SRNOM, as we observed in this study, enhanced the rate and extent of Cd-ferrihydrite microbial reduction, especially under high C/Fe ratios. We also conducted experiments using PPHA instead of SRNOM, and similar effects on Fe(III) reduction were observed, but the extent of reduction at similar C/Fe ratios was lower than with SRNOM ([Figure S1](#)).

Adsorbed NOM can affect microbial Fe(III) reduction in a range of ways including by covering the mineral surface, complexing of Fe atoms, changing aggregation properties or working as an electron shuttle, etc.^{20,25,36} To understand the potential cause of our observations, we evaluated the change of ferrihydrite aggregation by monitoring the sedimentation behavior of Cd-ferrihydrite associated with different amounts of SRNOM ([Figure S2](#)). Visual observation showed that adsorbed SRNOM decelerated ferrihydrite sedimentation which became more obvious at higher C/Fe ratios, suggesting the ferrihydrite aggregate size decreased and thus the available surface for bacterial electron transfer increased with higher SRNOM concentrations.²⁵ The increased Fe(III) reduction rate we observed in Cd-ferrihydrite associated with SRNOM at high C/Fe ratios could be partially explained by this observation as there was more available surface for microbial Fe(III) reduction.^{25,37} Additionally, adsorbed OM can help to transfer electrons between microbes and minerals,³⁸ but the dissolved fraction of NOM can further facilitate microbial Fe(III) reduction by working as an electron shuttle.³⁹ The remaining aqueous SRNOM measured at C/Fe ratios of 1.6 is 31 mgC/L ([Figure S3](#)), above the electron shuttling threshold (5 mgC/L) reported before;³⁹ thus, the dissolved NOM can shuttle the electrons between *G. sulfurreducens* and ferrihydrite leading to the faster rate of Fe(III) reduction. Additionally, the concentration of aqueous Cd and its toxicity to *G. sulfurreducens* should also be considered. An increased concentration of aqueous Cd could inhibit the activity of *G. sulfurreducens*, and thus decrease microbial Fe(III) reduction.¹⁵ More discussion on this can be found in the later section on Cd release into solution. Besides the factors discussed above, the presence of NOM could also alter the ferrihydrite transformation pathways and affect subsequent microbial Fe(III) reduction as different secondary Fe minerals have differences in bioavailability.⁴⁰ Ferrihydrite transformation itself may also remobilize associated Cd and change its toxicity

toward *G. sulfurreducens*. We therefore tracked Fe mineralogical changes to further this discussion.

Fe Mineralogical Changes. To explore the Fe mineralogical changes, the incubated aggregates of ferrihydrite with different amounts of cadmium and SRNOM were characterized with XRD and SEM, and selected ones were further characterized with Mössbauer spectroscopy. In the absence of Cd and SRNOM, the microbial ferrihydrite reduction resulted in the formation of magnetite as indicated by the XRD pattern (Figure 2a). The presence of Cd decreased Fe(III) reduction as shown in Figure 1b and led to the formation of lepidocrocite instead of magnetite.

SRNOM with a low C/Fe ratio (0.2) also facilitated lepidocrocite formation in the presence of Cd. The analysis of full width at half-maximum (fwhm) of the XRD pattern suggests no obvious difference in average crystallite size between lepidocrocite formed at C/Fe ratios of 0 and 0.2. In

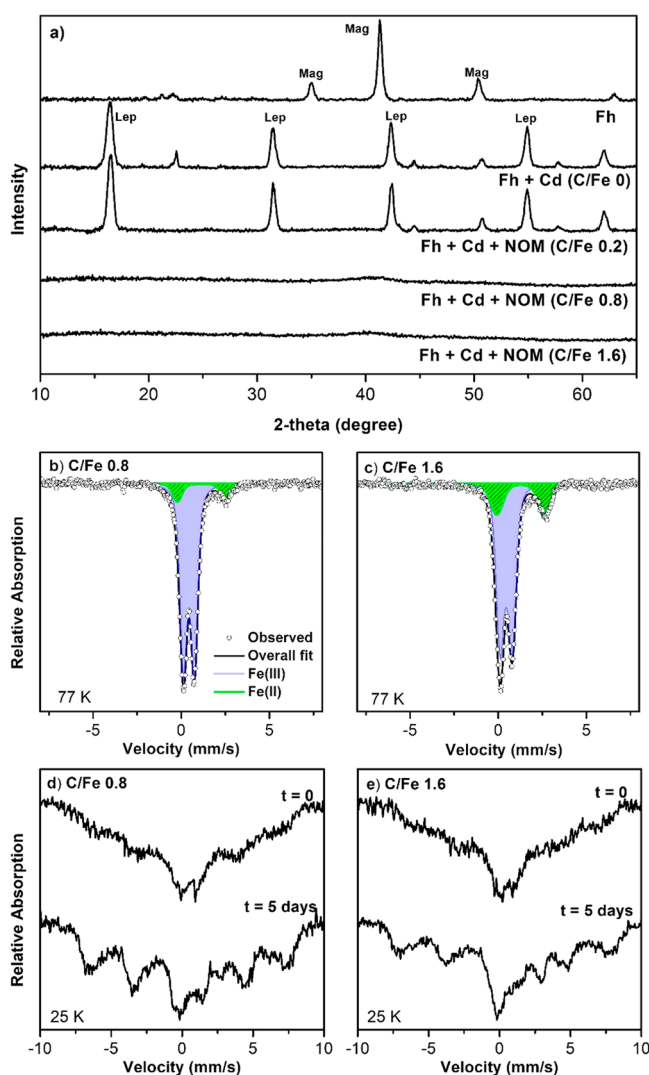


Figure 2. (a) X-ray diffraction patterns of ferrihydrite with different amounts of cadmium and SRNOM incubated with Fe(III)-reducing bacteria (*G. sulfurreducens*) for 5 days. (b) Mössbauer spectroscopy analysis of microbial reduced ferrihydrite with adsorbed Cd and SRNOM at a C/Fe ratio of 0.8 and (c) 1.6 for 5 days. The Mössbauer spectra collected at 25 K for ferrihydrite with adsorbed Cd and SRNOM at the C/Fe ratio of (d) 0.8 and (e) 1.6 before and after microbial reduction were also presented.

SEM images (Figure S4), tabular crystals were found with similar length and diameter for C/Fe ratios of 0 and 0.2, which is consistent with XRD results. A diffraction signal at 23 degrees (2theta) was found only in the experiments with a C/Fe ratio of 0 but not in experiments with a C/Fe ratio of 0.2. This diffraction signal may be related to the presence of a minor fraction of goethite as a secondary Fe mineral. Note that no goethite-like structures were found in any SEM image. However, considering that the XRD samples were dried in the glovebox over 1 week (not for SEM samples), goethite may have formed during this drying process.¹

At the high C/Fe ratios of 0.8 and 1.6, no diffraction signals were observed in the XRD patterns. In the SEM images, we also only observed amorphous structures in the solids after incubation, which were similar to the morphology of the initial solids (Figure S5). Both the XRD and SEM results suggest that no secondary Fe minerals were formed during microbial reduction of ferrihydrite at C/Fe ratios of 0.8 and 1.6.

⁵⁷Fe Mössbauer spectroscopy was also applied to further track the Fe mineralogical changes in samples at C/Fe ratios of 0.8 and 1.6. After 5 days of microbial incubation, a Fe(II) doublet emerged in addition to the Fe(III) doublet, indicating the reduction of ⁵⁷Fe(III) in ferrihydrite (Figure 2b,c). At the C/Fe ratio of 0.8, the site populations of Fe(II) doublet accounted for $10.6 \pm 0.9\%$ of the relative abundance which was similar to the result obtained by the wet-chemical ferrozine method ($12.0 \pm 2.0\%$). A higher percentage of Fe(II) was measured at the C/Fe ratio of 1.6, with $21.5 \pm 0.9\%$ relative area present as Fe(II), which was consistent with $23.5 \pm 1.9\%$ Fe(II) measured by the ferrozine method. The ratio of Fe(II)/Fe(III), a critical factor controlling ferrihydrite transformation,⁴¹ was comparably high in the solid phases, but no other secondary Fe minerals, i.e., lepidocrocite or goethite, were determined.

In Mössbauer spectra at 25 K, we found that SRNOM-Cd-ferrihydrite associations after microbial reduction were more magnetically ordered than the original associations (Figure 2d,e), indicating a higher degree of crystallinity, or stronger inter-Fe-particle interactions after microbial incubation. All samples before and after incubation were well ordered at 6 K (Figure S6) and the Mössbauer spectral parameters of the Fe(III) sextets (Table S3) were consistent with ferrihydrite before and after microbial incubation. The probability distribution of hyperfine fields for the different samples showed that different amounts of NOM did not lead to any difference in the hyperfine field distribution of the initial ferrihydrite. In our sedimentation study, we also did not observe an obvious difference between the C/Fe ratios of 0.8 and 1.6 (Figure S2). However, after microbial incubation, the hyperfine field at the C/Fe ratio of 0.8 was slightly higher, while at the C/Fe ratio of 1.6, it became more widely distributed, indicating the possible formation of some new short-range ordered Fe(III) (Figure S7). A similar hyperfine field distribution was recorded for a SRNOM-Fh coprecipitate,²⁹ suggesting the spatial distribution of Fe(III) and NOM may be altered by microbial incubation.

Cd Release into Solution. Considering its nanometer dimensions and abundant surface hydroxyl groups, ferrihydrite is regarded as a critical sorbent for Cd in the natural environment.⁴² In the abiotic control of this study, 67.4% of Cd was removed from the aqueous phase by 7 mM of ferrihydrite within 1 day and aqueous Cd stabilized at 3.68 ± 0.25 mg/L over 5 days. SRNOM at the C/Fe ratio of 0.2

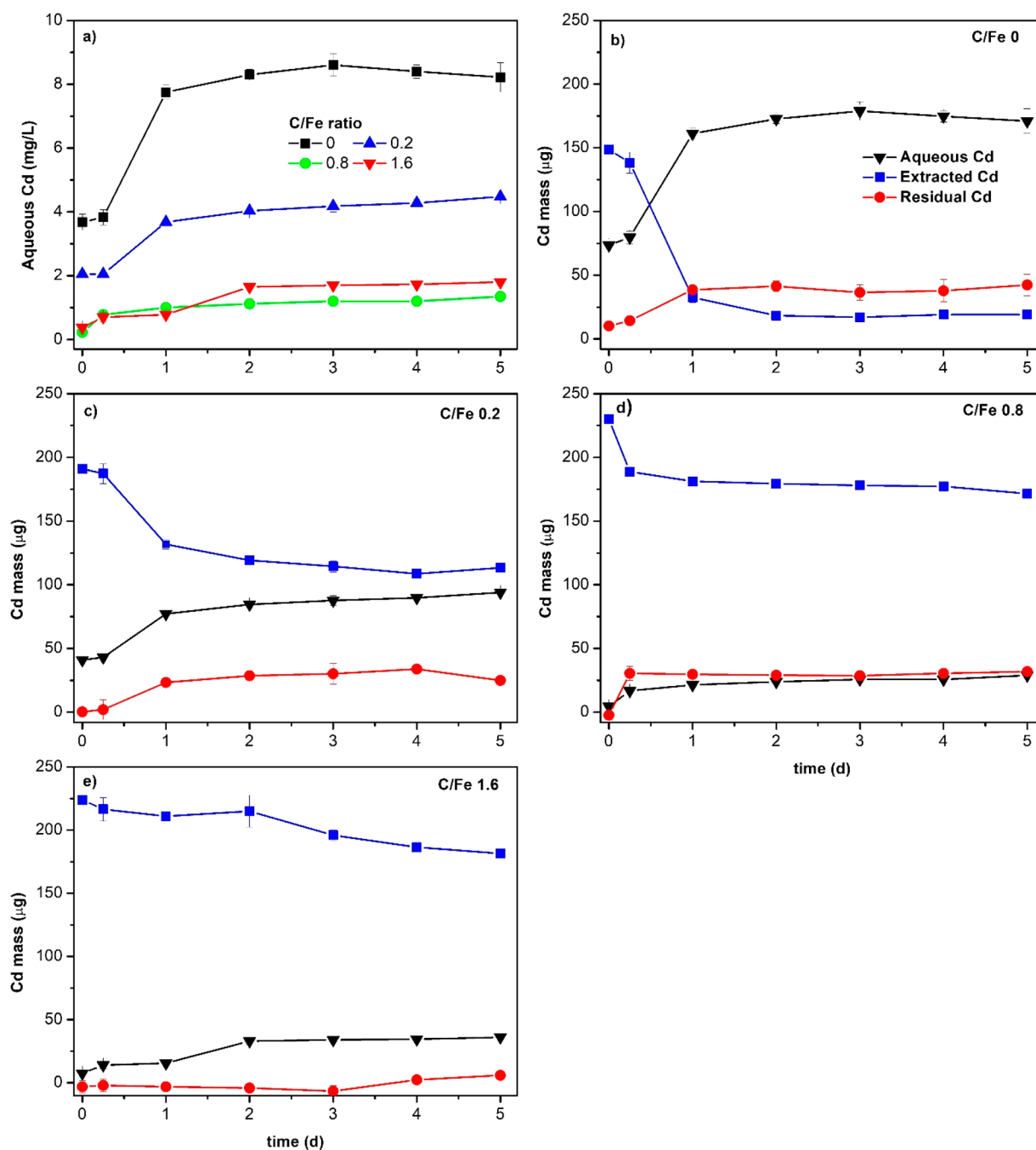


Figure 3. (a) Aqueous Cd concentration during microbial reduction (*G. sulfurreducens*) of Cd-ferrihydrite associated with different amounts of SRNOM. (b–e) Cd mass distribution during the incubation of Cd-ferrihydrite associated with different amounts of SRNOM. The mass distribution was calculated from Cd concentrations measured in different samples multiplied by the initial volume of the solution. Data plotted represent the mean and standard deviation in triplicate bottles.

decreased aqueous Cd concentration to 2.05 mg/L. Further increasing the C/Fe ratio to 0.8 or 1.6 resulted in Cd concentrations below 0.4 mg/L, indicating around 96.6–97.9% of Cd to be associated with the solid phase. In general, the presence of SRNOM improved the abiotic removal of Cd from the aqueous phase. This observation aligns with other studies where model organic ligand also enhanced Cd adsorption onto ferrihydrite and the formation of surface ternary complex was suggested.^{43,44}

During the microbial reduction with *G. sulfurreducens*, obvious Cd release was observed at a C/Fe ratio 0, with 61% of preadsorbed Cd released into aqueous phase over 1 day

(Figure 3a). Less Cd was released during microbial ferrihydrite reduction with increasing C/Fe ratios. At C/Fe ratio 0.8 and 1.6, only 5–10% of preadsorbed Cd was released over 5 days incubation even though enhanced microbial ferrihydrite reduction was observed. This different Cd release during microbial reduction can be partially explained by the diverse ferrihydrite transformation pathways at different C/Fe ratios. At low C/Fe ratios, ferrihydrite was transformed into lepidocrocite during the microbial incubation. Preadsorbed Cd can be first released into the aqueous phase due to the loss of binding sites in ferrihydrite, and then readsorbed by the newly formed secondary Fe minerals (e.g., lepidocrocite in this

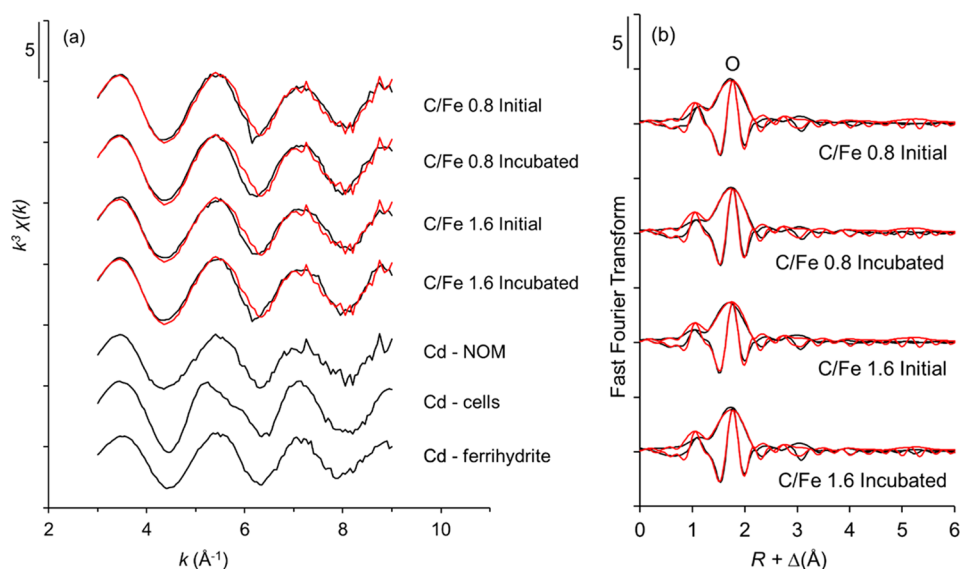


Figure 4. Cd k^3 -weighted EXAFS to a k of 9 (a) and their corresponding Fast Fourier Transform (b) of Cd-NOM-ferrihydrite association with a C/Fe ratio of 0.8 and 1.6 that were taken before and after microbial reduction (for 5 days) by *G. sulfurreducens*. Experimental and linear combination fit curves are depicted in black and red lines, respectively. The spectral components weighted by their fitted proportions for a k of 9 are reported in Table 1.

study). Considering that secondary Fe minerals normally have a larger particle size and less surface area than ferrihydrite,^{30,45} only part of the released Cd can be re-adsorbed resulting in an increase of Cd in the aqueous phase. Cd can also be reprecipitated with Fe(II) minerals formed under certain geochemical conditions, for example with siderite or vivianite.¹⁵ However, in our experiments, we did not have elevated concentrations of anions such as carbonate or phosphate present, so the effect of Fe(II) mineral formation is less important. Compared to the absence of NOM, the extent of Cd release at C/Fe ratio of 0.2 was lower, which can be related to the impeded ferrihydrite transformation and Cd bonding with adsorbed NOM.

At high C/Fe ratios, even though more Fe(III) was reduced, ferrihydrite transformation was inhibited. The lack of mineral transformation limited the relocation of adsorbed Cd and caused less Cd release to the aqueous phase. The decrease of the aqueous Cd concentration, however, decreased the exposure of Cd to *G. sulfurreducens*, thus enabling more prolonged microbial reduction. This is consistent with the observed continuous Fe(III) reduction after 6 h in setups with C/Fe ratios of 0.8 and 1.6, but not in setups with C/Fe ratios of 0 and 0.2 (Figure 1b). However, the inhibited ferrihydrite transformation cannot be the only reason for the impeded Cd release at high C/Fe ratios. There was $35 \pm 3\%$ of Fe(III) reduced at C/Fe ratio of 1.6 and around 1 mM Fe(II) released into solution (Figure 1), Cd may have lost abundant adsorption sites during the reductive Fe(III) dissolution, and the bonding between Cd and NOM could be critical in preventing Cd release into solution. To further this discussion, it is beneficial to investigate the Cd distribution in the solid phase before and after microbial reduction.

Cd Redistribution during Microbial Fe(III) Reduction.

To better investigate Cd redistribution during microbial incubation, we first applied chemical extraction (at pH 4.0) to determine the amount of Cd adsorbed to the solid phase. On the basis of the amount of extracted Cd, aqueous Cd and initially added Cd measured by MP-AES, we calculated the

amount of residual Cd in the solid after mild extraction and determined the Cd mass distribution in different phases (Figure 3b–e). The fraction of extractable Cd was also calculated by dividing the amount of extracted Cd with the sum of extracted and residual Cd to evaluate the stability of Cd in the solid phase.

In the absence of SRNOM, microbial reduction induced ferrihydrite transformation into lepidocrocite and released 61% of pre-adsorbed Cd into the aqueous phase. The remaining Cd in the solid became less susceptible to extraction over time, with extractable Cd decreased from $91 \pm 3\%$ over 6 h into $46 \pm 3\%$ over 1 day, and further decreased and maintained at about 30%. This increased stability of Cd remaining in the solid phase can be related to the formation of secondary Fe mineral as suggested in previous studies.^{15,46,47} The structural replacement of Fe(III) by Cd^{2+} was less likely considering that the atomic radius of Cd^{2+} (109 pm) is bigger than that of the Fe^{3+} ion (69 pm at low spin) in the crystal lattice.⁴⁸ However, ferrihydrite needs to aggregate before the transformation,^{28,46} during which some adsorbed Cd ($\sim 18\%$) can be enclosed within the aggregates and incorporated (not structural replacement) into the secondary Fe minerals thus improving its stability. At the C/Fe ratio of 0.2, the pH 4.0 extractable Cd only slightly decreased to $85 \pm 5\%$ after microbial reduction, indicating that most of the Cd was associated with the solid by adsorption. Even though we observed the formation of lepidocrocite in this experimental setup, the extent of ferrihydrite transformation was expected to decrease with increasing C/Fe ratio,⁴⁹ thus having less opportunity for the Cd to be enclosed during the ferrihydrite aggregation and transformation.

At the C/Fe ratio of 0.8, there was around 90% of extractable Cd in the solid, and nearly 100% at the C/Fe ratio of 1.6. Explaining how Cd redistributes during microbial reduction at these high C/Fe ratios was more challenging as Cd can not only associate with ferrihydrite but also bond with SRNOM. The Cd complexing capacity of dissolved NOM (not SRNOM) was reported as $1042 \mu\text{mol Cd g}^{-1} \text{C}$.⁵⁰ Even

Table 1. Results of the Cd K-edge EXAFS LC Fits to k of 9 for Cd-NOM-Fh Associations before and after Reduction by *G. sulfurreducens* for 5 Days

sample ID	Cd ~ Fh ^a	Cd ~ cells ^a	Cd-NOM ^a	sum	R-factor
C/Fe 0.8 initial	81 ± 6		19 ± 5	100	0.04913
C/Fe 0.8 incubated	41 ± 7	41 ± 8	18 ± 5	100	0.00468
C/Fe 1.6 initial	72 ± 5		28 ± 4	100	0.03631
C/Fe 1.6 incubated	50 ± 5	40 ± 8	10 ± 5	100	0.04386

^aThe proportions of the fitted components are given in % with their uncertainties. Contributions below 5% were considered to be not significant. The goodness of fit is estimated by $R\text{-factor} = \frac{\sum (y_{\text{measured}} - y_{\text{calculated}})^2}{\sum y_{\text{measured}}^2}$

though the value may change due to the variation of NOM composition, we only applied this value for a rough estimation and comparison. In the experiment with C/Fe ratios between 0.2 and 1.6, the Cd/C ratio was 5882–714 $\mu\text{mol Cd g}^{-1}\text{C}$. In the setup with a C/Fe ratio of 1.6, all of the Cd can therefore be bonded with NOM before its adsorption to ferrihydrite. Note Fe could also compete for the bonding sites in NOM thus impede the bonding between Cd and NOM. However, it is less likely that Cd is only associated with NOM and adsorbed onto ferrihydrite through Cd-NOM-ferrihydrite ternary complexes. We observed 78% of NOM was adsorbed by ferrihydrite at a C/Fe ratio of 1.6, but 97% of Cd was removed from solution, indicating the direct Cd association with ferrihydrite also occurred.

To further investigate Cd distribution between NOM, ferrihydrite, and biomass from microbes, we also characterized the solids with a C/Fe ratio of 0.8 and 1.6 before and after microbial incubation with EXAFS. The most satisfactory Linear Combination Fits (LCF) of the Cd K-edge EXAFS data were obtained using the following fitting components: Cd adsorbed to ferrihydrite, Cd adsorbed to *G. sulfurreducens* cells, and Cd complexed by NOM (Figure 4, Table S4). Due to the fragile nature of the organic rich samples under the beam of more than 26 000 eV, satisfying LC fits were only possible to a k of 9. Although for verification of the results, we also fitted the components to the k of 10 and 12, which are shown in the SI (Figure S8 and Table S5). LC fits to the k of 9, with supported trends by fits to the k of 10 and 12, indicate that before microbial reduction, Cd was more strongly bonded with ferrihydrite (81 ± 6%) than with NOM (19 ± 5%) at a C/Fe ratio 0.8, while the proportion of Cd bonded with NOM in the sample with C/Fe ratio of 1.6 slightly increased to 28 ± 4% (Table 1). After microbial reduction by *G. sulfurreducens*, Cd K-edge EXAFS indicates that approximately 41 ± 7% and 50 ± 5% of Cd was bonded with ferrihydrite at C/Fe ratios of 0.8 and 1.6, respectively. Shell-by-shell analysis also give evidence of Cd–O–Fe and Cd–O–C binding environments (Figure S9 and Table S6). The result showed Cd in the solid phase was redistributed after microbial reduction with a decreased proportion of Cd bonded with ferrihydrite.

In the fitting results, the Cd-cells bond took a large proportion (40–41%) after microbial reduction at C/Fe ratio of 0.8 and 1.6, but note it is very challenging to differentiate the Cd bond between SRNOM and biomass from cells by XAS, as both of the OMs are enriched in carboxylic groups that can strongly associate with Cd.^{51,52} Considering that the same amount of cells were added to all setups and a large proportion of preadsorbed Cd released at C/Fe ratio of 0 and 0.2 during microbial reduction, the Cd bond with biomass from cells cannot explain the decreased Cd release at high C/Fe ratios. The extra carboxylic group coming with SRNOM (increasing C/Fe ratios) and its bonding with Cd may better explain the

impeded Cd release at the C/Fe ratio of 0.8 and 1.6. During microbial ferrihydrite reduction, ferrihydrite bonded Cd can be first released and then recaptured by NOM. The Cd-NOM association could be flocculated with Fe(II) or Fe(III) ions (the Fe(III) can be formed from Fe(II) after donating electrons to NOM), thus preventing the release of Cd and adsorbed SRNOM. The negligible release of SRNOM and Cd after microbial Fe(III) reduction observed in this study is consistent with this hypothesis. In addition, the changed Fe(III) and NOM distribution suggested by Mössbauer spectroscopy (Figure S7) also supports the hypothesis of Fe(III) and NOM flocculating during microbial reduction.

ENVIRONMENTAL IMPLICATIONS

Microbial Fe(III) reduction is known to affect the fate of Cd bound to Fe minerals and can threaten soil and groundwater safety.^{18,53} However, it becomes more complicated to predict the fate of Cd in the presence of NOM. In this study, we have shown that NOM can enhance the extent and rate of microbial ferrihydrite reduction, but inhibited ferrihydrite transformation and limited Cd release, thus making it beneficial for decreasing the mobility of Cd under reducing conditions.

The result of our study also has important implications from the perspective of environmental engineering. Ferrihydrite, as a cheap, reactive nanomaterial, shows great potential for in situ remediation and wastewater treatment but its poor stability has limited its application at large scale. This study shows that the coating of NOM to ferrihydrite can not only increase the abiotic adsorption of Cd but also inhibit ferrihydrite transformation and improve the long-term stability of associated Cd under reducing environments. It suggests a possible direction for the modification of ferrihydrite to improve its use as an environmentally engineered nanomaterial.

ASSOCIATED CONTENT


Supporting Information

The Supporting Information is available free of charge at <https://pubs.acs.org/doi/10.1021/acs.est.0c03062>.

Details about X-ray absorption spectroscopy analysis, Mössbauer spectroscopy, SEM images, NOM characterization, and data of the set-ups with PPHA (PDF)

AUTHOR INFORMATION

Corresponding Author

Zhe Zhou – Geomicrobiology, Center for Applied Geosciences, University of Tuebingen, 72076 Tuebingen, Germany;
 orcid.org/0000-0001-7732-9582; Email: zhe_research@outlook.com

Authors

E. Marie Muehe – Geomicrobiology, Center for Applied Geosciences, University of Tuebingen, 72076 Tuebingen, Germany

Elizabeth J. Tomaszewski – Geomicrobiology, Center for Applied Geosciences, University of Tuebingen, 72076 Tuebingen, Germany; Delaware Environmental Institute, University of Delaware, Newark, Delaware 19716, United States

Juan Lezama-Pacheco – Department of Environmental Earth System Science, Stanford University, Stanford, California 94305, United States

Andreas Kappler – Geomicrobiology, Center for Applied Geosciences, University of Tuebingen, 72076 Tuebingen, Germany; orcid.org/0000-0002-3558-9500

James M. Byrne – Geomicrobiology, Center for Applied Geosciences, University of Tuebingen, 72076 Tuebingen, Germany; School of Earth Sciences, University of Bristol, Bristol BS8 1QU, United Kingdom; orcid.org/0000-0002-4399-7336

Complete contact information is available at:
<https://pubs.acs.org/10.1021/acs.est.0c03062>

Notes

The authors declare no competing financial interest.

ACKNOWLEDGMENTS

This work was supported by a DFG Grant KA 1736/55-1. We thank C. Reith, T. Bayer, J. Sorwat, S. Drabesch, and N. Jakus for assistance with sample analysis. We also want to thank R. Davis and M. Latimer for XAS support at SSRL (beamline 11-2, proposal number 5263). Use of the Stanford Synchrotron Radiation Lightsource, SLAC National Accelerator Laboratory, is supported by the U.S. Department of Energy, Office of Science, Office of Basic Energy Sciences under Contract No. DE-AC02-76SF00515. The SSRL Structural Molecular Biology Program is supported by the DOE Office of Biological and Environmental Research, and by the National Institutes of Health, National Institute of General Medical Sciences (including P41GM103393). The contents of this publication are solely the responsibility of the authors and do not necessarily represent the official views of NIGMS or NIH.

REFERENCES

- (1) Cornell, R. M.; Schwertmann, U. *The Iron Oxides: Structure, Properties, Reactions, Occurrences and Uses*; John Wiley & Sons: 2003.
- (2) Schwertmann, U. t.; Fischer, W. Natural “amorphous” ferric hydroxide. *Geoderma* **1973**, *10* (3), 237–247.
- (3) UNEP. Final review of scientific information on cadmium. 2010.
- (4) Randall, S.; Sherman, D.; Ragnarsdottir, K.; Collins, C. R. The mechanism of cadmium surface complexation on iron oxyhydroxide minerals. *Geochim. Cosmochim. Acta* **1999**, *63* (19–20), 2971–2987.
- (5) Rosenfeld, C. E.; Chaney, R. L.; Martinez, C. E. Soil geochemical factors regulate Cd accumulation by metal hyperaccumulating *Noccaea caerulea* (J. Presl & C. Presl) FK Mey in field-contaminated soils. *Sci. Total Environ.* **2018**, *616*, 279–287.
- (6) Hansel, C. M.; Benner, S. G.; Neiss, J.; Dohnalkova, A.; Kukkadapu, R. K.; Fendorf, S. Secondary mineralization pathways induced by dissimilatory iron reduction of ferrihydrite under advective flow. *Geochim. Cosmochim. Acta* **2003**, *67* (16), 2977–2992.
- (7) Boland, D. D.; Collins, R. N.; Miller, C. J.; Glover, C. J.; Waite, T. D. Effect of solution and solid-phase conditions on the Fe (II)-accelerated transformation of ferrihydrite to lepidocrocite and goethite. *Environ. Sci. Technol.* **2014**, *48* (10), 5477–5485.
- (8) Eusterhues, K.; Hädrich, A.; Neidhardt, J.; Küsel, K.; Keller, T.; Jandt, K.; Totsche, K. Reduction of ferrihydrite with adsorbed and coprecipitated organic matter: microbial reduction by *Geobacter bremensis* vs. abiotic reduction by Na-dithionite. *Biogeochemistry* **2014**, *11* (18), 4953.
- (9) Wolf, M.; Kappler, A.; Jiang, J.; Meckenstock, R. U. Effects of humic substances and quinones at low concentrations on ferrihydrite reduction by *Geobacter metallireducens*. *Environ. Sci. Technol.* **2009**, *43* (15), 5679–5685.
- (10) Aeppli, M.; Kaegi, R.; Kretzschmar, R.; Voegelin, A.; Hofstetter, T. B.; Sander, M. Electrochemical analysis of changes in iron oxide reducibility during abiotic ferrihydrite transformation into goethite and magnetite. *Environ. Sci. Technol.* **2019**, *53* (7), 3568–3578.
- (11) Shimizu, M.; Zhou, J.; Schröder, C.; Obst, M.; Kappler, A.; Borch, T. Dissimilatory reduction and transformation of ferrihydrite-humic acid coprecipitates. *Environ. Sci. Technol.* **2013**, *47* (23), 13375–13384.
- (12) Peretyazhko, T.; Sposito, G. Iron (III) reduction and phosphorous solubilization in humid tropical forest soils. *Geochim. Cosmochim. Acta* **2005**, *69* (14), 3643–3652.
- (13) Tronc, E.; Belleville, P.; Jolivet, J. P.; Livage, J. Transformation of ferric hydroxide into spinel by Fe(II) adsorption. *Langmuir* **1992**, *8* (1), 313–319.
- (14) Li, C.; Yi, X.; Dang, Z.; Yu, H.; Zeng, T.; Wei, C.; Feng, C. Fate of Fe and Cd upon microbial reduction of Cd-loaded polyferric flocs by *Shewanella oneidensis* MR-1. *Chemosphere* **2016**, *144*, 2065–2072.
- (15) Muehe, E. M.; Obst, M.; Hitchcock, A.; Tyliczszak, T.; Behrens, S.; Schröder, C.; Byrne, J. M.; Michel, F. M.; Krämer, U.; Kappler, A. Fate of Cd during Microbial Fe(III) Mineral Reduction by a Novel and Cd-Tolerant *Geobacter* Species. *Environ. Sci. Technol.* **2013**, *47* (24), 14099–14109.
- (16) Muehe, E. M.; Adaktylou, I. J.; Obst, M.; Zeitvogel, F.; Behrens, S.; Planer-Friedrich, B.; Kraemer, U.; Kappler, A. Organic carbon and reducing conditions lead to cadmium immobilization by secondary Fe mineral formation in a pH-neutral soil. *Environ. Sci. Technol.* **2013**, *47* (23), 13430–13439.
- (17) Lin, X.; Burns, R. C.; Lawrance, G. A. Effect of cadmium (II) and anion type on the ageing of ferrihydrite and its subsequent leaching under neutral and alkaline conditions. *Water, Air, Soil Pollut.* **2003**, *143* (1–4), 155–177.
- (18) Zhang, C.; Ge, Y.; Yao, H.; Chen, X.; Hu, M. Iron oxidation-reduction and its impacts on cadmium bioavailability in paddy soils: a review. *Front. Environ. Sci. Eng.* **2012**, *6* (4), 509–517.
- (19) Lalonde, K.; Mucci, A.; Ouellet, A.; Gelinas, Y. Preservation of organic matter in sediments promoted by iron. *Nature* **2012**, *483* (7388), 198–200.
- (20) Poggenburg, C.; Mikutta, R.; Schippers, A.; Dohrmann, R.; Guggenberger, G. Impact of natural organic matter coatings on the microbial reduction of iron oxides. *Geochim. Cosmochim. Acta* **2018**, *224*, 223–248.
- (21) Schwertmann, U.; Wagner, F.; Knicker, H. Ferrihydrite-humic associations. *Soil Sci. Soc. Am. J.* **2005**, *69* (4), 1009–1015.
- (22) Jones, A. M.; Collins, R. N.; Rose, J.; Waite, T. D. The effect of silica and natural organic matter on the Fe(II)-catalysed transformation and reactivity of Fe(III) minerals. *Geochim. Cosmochim. Acta* **2009**, *73* (15), 4409–4422.
- (23) Nevin, K. P.; Lovley, D. R. Mechanisms for Fe (III) oxide reduction in sedimentary environments. *Geomicrobiol. J.* **2002**, *19* (2), 141–159.
- (24) Royer, R. A.; Burgos, W. D.; Fisher, A. S.; Jeon, B.-H.; Unz, R. F.; Dempsey, B. A. Enhancement of hematite bioreduction by natural organic matter. *Environ. Sci. Technol.* **2002**, *36* (13), 2897–2904.
- (25) Amstaetter, K.; Borch, T.; Kappler, A. Influence of humic acid imposed changes of ferrihydrite aggregation on microbial Fe (III) reduction. *Geochim. Cosmochim. Acta* **2012**, *85*, 326–341.
- (26) Lovley, D. R.; Coates, J. D.; Blunt-Harris, E. L.; Phillips, E. J.; Woodward, J. C. Humic substances as electron acceptors for microbial respiration. *Nature* **1996**, *382* (6590), 445.

- (27) Bauer, I.; Kappler, A. Rates and extent of reduction of Fe (III) compounds and O₂ by humic substances. *Environ. Sci. Technol.* **2009**, *43* (13), 4902–4908.
- (28) ThomasArrigo, L. K.; Kaegi, R.; Kretzschmar, R. Ferrihydrite Growth and Transformation in the Presence of Ferrous Iron and Model Organic Ligands. *Environ. Sci. Technol.* **2019**, *53* (23), 13636–13647.
- (29) Zhou, Z.; Latta, D. E.; Noor, N.; Thompson, A.; Borch, T.; Scherer, M. M. Fe(II)-Catalyzed Transformation of Organic Matter-Ferrihydrite Coprecipitates: A Closer Look Using Fe Isotopes. *Environ. Sci. Technol.* **2018**, *52* (19), 11142–11150.
- (30) Schwertmann, U.; Cornell, R. M. *Iron Oxides in the Laboratory: Preparation and Characterization*; John Wiley & Sons: 2008.
- (31) Notini, L.; Byrne, J. M.; Tomaszewski, E. J.; Latta, D. E.; Zhou, Z.; Scherer, M. M.; Kappler, A. Mineral Defects Enhance Bioavailability of Goethite toward Microbial Fe(III) Reduction. *Environ. Sci. Technol.* **2019**, *53* (15), 8883–8891.
- (32) Porsch, K.; Kappler, A. FeII oxidation by molecular O₂ during HCl extraction. *Environmental Chemistry* **2011**, *8* (2), 190–197.
- (33) Stookey, L. L. Ferrozine—a new spectrophotometric reagent for iron. *Anal. Chem.* **1970**, *42* (7), 779–781.
- (34) Wang, G.-S.; Hsieh, S.-T. Monitoring natural organic matter in water with scanning spectrophotometer. *Environ. Int.* **2001**, *26* (4), 205–212.
- (35) Rancourt, D.; Ping, J. Voigt-based methods for arbitrary-shape static hyperfine parameter distributions in Mössbauer spectroscopy. *Nucl. Instrum. Methods Phys. Res., Sect. B* **1991**, *58* (1), 85–97.
- (36) Nevin, K. P.; Lovley, D. R. Mechanisms for Fe(III) Oxide Reduction in Sedimentary Environments. *Geomicrobiol. J.* **2002**, *19* (2), 141–159.
- (37) Lv, J.; Zhang, S.; Wang, S.; Luo, L.; Cao, D.; Christie, P. Molecular-scale investigation with ESI-FT-ICR-MS on fractionation of dissolved organic matter induced by adsorption on iron oxyhydroxides. *Environ. Sci. Technol.* **2016**, *50* (5), 2328–2336.
- (38) Marsili, E.; Baron, D. B.; Shikhare, I. D.; Coursolle, D.; Gralnick, J. A.; Bond, D. R. Shewanella secretes flavins that mediate extracellular electron transfer. *Proc. Natl. Acad. Sci. U. S. A.* **2008**, *105* (10), 3968–3973.
- (39) Jiang, J.; Kappler, A. Kinetics of Microbial and Chemical Reduction of Humic Substances: Implications for Electron Shuttling. *Environ. Sci. Technol.* **2008**, *42* (10), 3563–3569.
- (40) Aeppli, M.; Vranic, S.; Kaegi, R.; Kretzschmar, R.; Brown, A. R.; Voegelin, A.; Hofstetter, T. B.; Sander, M. Decreases in Iron Oxide Reducibility during Microbial Reductive Dissolution and Transformation of Ferrihydrite. *Environ. Sci. Technol.* **2019**, *53* (15), 8736–8746.
- (41) Pedersen, H. D.; Postma, D.; Jakobsen, R.; Larsen, O. Fast transformation of iron oxyhydroxides by the catalytic action of aqueous Fe(II). *Geochim. Cosmochim. Acta* **2005**, *69* (16), 3967–3977.
- (42) Davies-Colley, R. J.; Nelson, P. O.; Williamson, K. J. Copper and cadmium uptake by estuarine sedimentary phases. *Environ. Sci. Technol.* **1984**, *18* (7), 491–499.
- (43) Song, Y.; Swedlund, P. J.; Singhal, N.; Swift, S. Cadmium(II) Speciation in Complex Aquatic Systems: A Study with Ferrihydrite, Bacteria, and an Organic Ligand. *Environ. Sci. Technol.* **2009**, *43* (19), 7430–7436.
- (44) Song, Y.; Swedlund, P. J.; Singhal, N. Copper(II) and Cadmium(II) Sorption onto Ferrihydrite in the Presence of Phthalic Acid: Some Properties of the Ternary Complex. *Environ. Sci. Technol.* **2008**, *42* (11), 4008–4013.
- (45) Vu, H. P.; Shaw, S.; Brinza, L.; Benning, L. G. Partitioning of Pb (II) during goethite and hematite crystallization: Implications for Pb transport in natural systems. *Appl. Geochem.* **2013**, *39*, 119–128.
- (46) Banfield, J. F.; Welch, S. A.; Zhang, H.; Ebert, T. T.; Penn, R. L. Aggregation-based crystal growth and microstructure development in natural iron oxyhydroxide biomineralization products. *Science* **2000**, *289* (5480), 751–754.
- (47) Huang, Y.; Zhang, S.; Liu, C.; Lu, H.; Ni, S.; Cheng, X.; Long, Z.; Wang, R. Transformations of 2-line ferrihydrite and its effect on cadmium adsorption. *Environ. Sci. Pollut. Res.* **2018**, *25* (18), 18059–18070.
- (48) Shannon, R. D. Revised effective ionic radii and systematic studies of interatomic distances in halides and chalcogenides. *Acta Crystallogr., Sect. A: Cryst. Phys., Diffr., Theor. Gen. Crystallogr.* **1976**, *32* (5), 751–767.
- (49) Chen, C. M.; Kukkadapu, R.; Sparks, D. L. Influence of Coprecipitated Organic Matter on Fe-(aq)(2+)-Catalyzed Transformation of Ferrihydrite: Implications for Carbon Dynamics. *Environ. Sci. Technol.* **2015**, *49* (18), 10927–10936.
- (50) Kaschl, A.; Römheld, V.; Chen, Y. Cadmium binding by fractions of dissolved organic matter and humic substances from municipal solid waste compost. *Journal of environmental quality* **2002**, *31* (6), 1885–1892.
- (51) Society, I. H. S. Elemental Compositions and Stable Isotopic Ratios of IHSS Samples. (May 16, **2018**).
- (52) Beveridge, T. J. Role of cellular design in bacterial metal accumulation and mineralization. *Annu. Rev. Microbiol.* **1989**, *43* (1), 147–171.
- (53) Suda, A.; Makino, T. Functional effects of manganese and iron oxides on the dynamics of trace elements in soils with a special focus on arsenic and cadmium: a review. *Geoderma* **2016**, *270*, 68–75.